Ciência e Agrotecnologia
SCIENCE AND AGROTECHNOLOGY

Ciência e Agrotecnologia, 47:e018722, 2023
http://dx.doi.org/10.1590/1413-7054202347018722

Food Science and Technology
eISSN 1981-1829

Solubility of different salts used in the control of the water activity of foods

Solubilidade de diferentes sais usados no controle da atividade de água de alimentos

Maria Julia Neves Martins[1], Marcio Augusto Ribeiro Sanches[1], Tiago Carregari Polachini[1], Eduardo Basílio de Oliveira[2], Jane Selia dos Reis Coimbra[2*], Javier Telis-Romero[1]

[1]Universidade Estadual Paulista/Unesp, Departamento de Engenharia e Tecnologia de Alimentos, Instituto de Biociências, Letras e Ciências Exatas/Ibilce, Campus São José do Rio Preto, SP, Brasil
[2]Universidade Federal de Viçosa/UFV, Departamento de Tecnologia de Alimentos/DTA, Equipe de Estudos de Materiais Alimentares/E²MA, Viçosa, MG, Brasil
*Corresponding author: jcoimbra@ufv.br

Received in December 15, 2022 and approved in April 5, 2023

ABSTRACT

Saturated salt solutions produce environments with specific relative humidities used in several applications, such as determining water sorption isotherms of foods. However, the preparation of saturated solutions requires knowledge of solubility data. Thus, the objective of this work was to determine the solubility of 14 salts: lithium bromide (LiBr), lithium chloride (LiCl), lithium iodide (LiI), magnesium chloride ($MgCl_2$), sodium iodide (NaI), potassium carbonate (K_2CO_3), magnesium nitrate ($Mg(NO_3)_2$), sodium bromide (NaBr), potassium iodide (KI), sodium chloride (NaCl), ammonium sulfate ($(NH_4)_2SO_4$), potassium chloride (KCl), potassium nitrate (KNO_3), and potassium sulfate (K_2SO_4) in the temperature range of 275.15 to 363.15 K at 101.3 kPa. The apparatus for the solubility determination consists of a jacketed glass cell and a magnetic stirrer. Furthermore, polynomial and exponential empirical models were fitted to the observed data to determine salt solubilities. Salt solubilities ranged from 7.39 to 80.41 g of salt·(100 g of solution)$^{-1}$. Sodium iodide (NaI) presented the highest ($p<0.05$) solubility, up to 343.15 K, and lithium iodide (LiI) up to 363.15 K. The specific equilibrium moistures afforded by saturated saline solutions were associated with water activity data. A general mathematical model to determine the solubility of different salts was not obtained because the dissolution behaviors of each salt are distinct. However, the availability of solubility data of saline solutions covering a wide range of temperatures is helpful since the salts have different behavior.

Index terms: Gravimetric method; exponential model; polynomial model; saturation; temperature.

RESUMO

Soluções salinas saturadas produzem ambientes com umidades relativas específicas utilizadas em diversas aplicações, como na determinação de isotermas de sorção de água de alimentos. No entanto, a preparação de soluções saturadas requer conhecimento de dados de solubilidade. Assim, o objetivo deste trabalho foi determinar a solubilidade de 14 sais: brometo de lítio (LiBr), cloreto de lítio (LiCl), iodeto de lítio (LiI), cloreto de magnésio ($MgCl_2$), iodeto de sódio (NaI), carbonato de potássio (K_2CO_3), nitrato de magnésio ($Mg(NO_3)_2$), brometo de sódio (NaBr), iodeto de potássio (KI), cloreto de sódio (NaCl), sulfato de amônio ($(NH_4)_2SO_4$), cloreto de potássio (KCl), nitrato de potássio (KNO_3) e sulfato de potássio (K_2SO_4) na faixa de temperatura de 275,15 a 363,15 K a 101,3 kPa. O aparelho para a determinação da solubilidade consiste em uma célula de vidro encamisada e um agitador magnético. Além disso, modelos empíricos polinomiais e exponenciais foram ajustados aos dados observados para determinar solubilidades de sal. A solubilidade do sal varia de 7,39 a 80,41 g de sal·(100 g de solução)$^{-1}$. Iodeto de sódio (NaI) apresentou o maior ($p<0.05$) solubilidade, até 343,15 K, e iodeto de lítio (LiI) até 363,15 K. Específicas umidades de equilíbrio proporcionadas pelas soluções salinas saturadas foram associadas aos dados de atividade de água. Um modelo matemático geral para determinar a solubilidade de diferentes sais não foi obtido porque os comportamentos de dissolução de cada sal são distintos. No entanto, a disponibilidade de dados de solubilidade de soluções salinas cobrindo uma ampla faixa de temperaturas é útil, pois os sais têm comportamento diferente.

Termos para indexação: Método gravimétrico; modelo exponencial; modelo polinomial; saturação; temperatura.

INTRODUCTION

Solubility is a physical property of matter, defined as the maximum quantity of a given solute dissolved in a solvent at a specific temperature and pressure. Solubility is affected by (1) the system characteristics, such as temperature, pressure, pH, and presence of compounds other than the solute and solvent. Usually, endothermic dissolution shows increased solubility

All the contents of this journal, except where otherwise noted, is licensed under a Creative Commons Attribution BY.

with increasing temperature, which may be associated with chemical structure reorganizing and changing the entropy (Martínez; Peña; Bustamante, 2011); (2) the natures of the solute and the solvent, such as molecular mass, size, molecular structure, polarity, quantity, and energy relationship through intermolecular interactions (Bhattachar; Deschenes; Wesley, 2006; Filippa; Gasull, 2014). According to the solute content, solutions are classified as saturated (contains the maximum quantity of a solute dissolved in a solvent), unsaturated or diluted (contains less dissolved solute than its saturation concentration), and supersaturated (contains more dissolved solute than its saturation concentration). Systems under supersaturated conditions tend to be unstable.

Farelo, Brachel and Offermann (1993) determined solubility data of NaCl and KCl aqueous ternary solutions from 293 K to 360 K. Pinho and Macedo (1996) described NaCl and KCl solubility data in water/methanol and water/ethanol systems at 298.15, 323.15, and 348.15 K. Wagner et al. (1998) measured the solubility of NaCl in organic solvents and aqueous solutions of organic solvents at 298.15 K. Thus, to the best of our knowledge, the solubility values of saline solutions for several types of salts over broad temperature ranges are scarce or obsolete in open-access literature.

Salts are used as solutes in several industrial formulations, and thus, knowledge of the solubility of different salts has many practical applications in various unit operations processes, such as crystallization, liquid–liquid extraction, and extractive or azeotropic distillation (Pinho; Macedo, 1996). The literature reported the application of saturated salt solutions to simulate environments with different relative humidities and to control the water activity of foods, as follows. For instance, Mali et al. (2005) evaluated the effect of adding plasticizers (glycerol and sorbitol) to cassava starch films on water sorption at relative humidities of 32, 58, 75, and 90%. Saturated NaCl solutions are widely used to evaluate the kinetics of water vapor sorption in biodegradable materials (Ribeiro Sanches et al., 2021). Larotonda et al. (2005) determined the water vapor permeability of Kraft paper impregnated with starch acetate under three relative humidity ranges (0 to 33%; 33 to 62%; 62 to 90%). Saline solutions of NaCl, KCl and $MgCl_2$ were applied in meat salting to analyze their effect on the water retention capacity and the diffusion coefficient in a food product (Bampi et al., 2016; Inguglia et al., 2017; Sanches et al., 2021; Zhang et al., 2020). Solutions of KCl and $MgCl_2$ are investigated as substitutes for NaCl in foods with the aim of sodium reduction.

Saline solutions are also used to obtain water sorption isotherms, described by the relationship between equilibrium moisture and food water activity under constant temperature and pressure conditions (Arslan-Tontul, 2020; Freitas et al., 2016). Knowledge and understanding of moisture sorption isotherms play a role in food science and engineering. Isotherms can help determine the shelf life of foods, estimate and predict their microbiological and chemical behavior, choose suitable packaging, and estimate and predict the physical stability of foods under known storage conditions (Leonardo Betiol et al., 2020; Polachini et al., 2016; Rosa et al., 2021; Silva et al., 2021).

The systematic method used to determine moisture sorption isotherms is the differential method, a static gravimetric method. The sample is subjected to increasing or decreasing relative humidity environments in the method, and the water content is measured after equilibration (Polachini et al., 2016). In the differential method, several relative humidity environments, under controlled conditions, are generated using different saturated salt solutions or sulfuric acid. However, sulfuric acid can promote changes in the concentration of the solution. In addition, sulfuric acid requires handling care since it is very corrosive, especially in low water activities, and solution splashes need to be avoided on the studied material. Thus, saturated salt solutions are considered most suitable for controlling the relative humidity environment because they can release or adsorb water without changing the relative humidity environment of equilibrium (Chirife; Resnik, 1984). It should be emphasized that solutions must be prepared from salt solubility data at the isotherm temperature because the solubilities of many salts vary with temperature, and the water activity of an apparent saturated solution can induce process errors.

Several saturated saline solutions perform distinctly concerning solubility due to differences in the molecular masses of salts and their behavior at the operating temperature (Martins et al., 2021; Martins et al., 2020; Ramya; Jain, 2017), highlighting the importance of evaluating the individual solubility of various types of salts. Despite the relevance of solubility for different salts, either under saturation conditions or at the solubility threshold, to obtain sorption isotherms accurately, the data are scarce and dispersed in the literature (Alberto Alves-Junior et al., 2021; Pinho; Macedo, 1996), and they were also measured at a reduced temperature range. To contribute to filling this gap and form a specific data bank for isotherms with salts commonly applied in the food industry over a wide temperature range, the objectives of this work were (*a*) to investigate the solubility of 14 saturated salt solutions, LiBr, LiCl, LiI, $MgCl_2$, NaI, K_2CO_3, $Mg(NO_3)_2$, NaBr, KI, NaCl, $(NH_4)_2SO_4$, KCl, KNO_3, and K_2SO_4, in aqueous medium at different temperatures (275.15 to 363.15 K) to provide a solubility database of different salts to be used in the construction of sorption isotherms; (*b*) to adjust empirical mathematical models to the experimental solubility data to obtain predictive equations for the various salts, and (*c*) to show the dependence of the solubility of the aforementioned salts at 11 temperature values (275.15 K, 278.15, 283.15, 293.15, 303.15, 313.15, 323.15, 333.15, 343.15, 353.15, and 363.15 K), which comprise the most ordinary temperature conditions of storage (275.15 to 313.15 K) and drying (323.15 to 363.15 K) of foods.

MATERIAL AND METHODS

Preparation of saline solutions

Saline solutions were prepared with 14 types of salts acquired from Sigma–Aldrich (St. Louis, MO, USA): LiBr, LiCl, LiI, $MgCl_2$, NaI, K_2CO_3, $Mg(NO_3)_2$, NaBr, KI, NaCl, $(NH_4)_2SO_4$, KCl, KNO_3, and K_2SO_4. Table 1 presents the chemical specifications.

Distilled (Marconi, model MA078/10) and deionized water (Marconi model MA3401) was used as the solvent with an electrical conductivity of 0.113 ± 0.004 μS·cm, thermal conductivity of 0.618 ± 0.002 $W \cdot m^{-1} \cdot K^{-1}$, and a measured specific resistance of 8.85 MΩ·cm.

Determination of salt solubility data

Salt solubility was determined in triplicate according to the methodology described by Martins et al. (2021) for the 14 studied salts at 11 temperature values (275.15 K, 278.15, 283.15, 293.15, 303.15, 313.15, 323.15, 333.15, 343.15, 353.15, and 363.15 K with a variation of ± 0.20 K). This temperature range simulates the conditions of storage (275.15 to 313.15 k) and drying (323.15 to 363.15 K) that are commonly used to determine water sorption isotherms of foods.

The experimental apparatus includes a glass cell, a thermocouple, an ultrathermostatic bath (Marconi, model MA-184), a stirrer, and a data acquisition system, as depicted in Figure 1.

The glass cell of 50 mL capacity is equipped with a water-circulating jacket to ensure an isothermal system. The cell contains two lateral inlets, one for solute feeding in the system and the other for taking samples and a top opening sealed with a Teflon stopper to prevent evaporation. The type K thermocouple (MT-455, Minipa, USA) was placed upon the sealed device in the center of the cell.

Table 1: Salt composition and supplier.

Chemical name	Chemical formula	Supplier	Purity (%)*	CAS number
Lithium bromide	LiBr	Sigma-Aldrich	≥ 99.9	7550-35-8
Lithium chloride	LiCl	Sigma-Aldrich	≥ 99.9	7447-41-8
Lithium iodide	LiI	Sigald (Sigma-Aldrich)	99.99	10377-51-2
Magnesium chloride	$MgCl_2$	Sigma (Sigma-Aldrich)	99.99	7786-30-3
Sodium iodide	NaI	Sigma-Aldrich	99.99	7681-82-5
Potassium carbonate	K_2CO_3	Sigald (Sigma-Aldrich)	99.99	584-08-7
Magnesium nitrate	$Mg(NO_3)_2$	Sigma-Aldrich	≥ 99.99	10377-60-3
Sodium bromide	NaBr	Sigma-Aldrich	≥ 99.99	7647-15-6
Potassium iodide	KI	Sigma-Aldrich	≥ 99.99	7681-11-0
Sodium chloride	NaCl	Sigma-Aldrich	≥ 99.5	7647-14-5
Ammonium sulfate	$(NH_4)_2SO_4$	Sigald (Sigma-Aldrich)	≥ 99.0	7783-20-2
Potassium chloride	KCl	Sigma-Aldrich	≥ 99.5	7447-40-7
Potassium nitrate	KNO_3	Sigald (Sigma-Aldrich)	≥ 99.0	7757-79-1
Potassium sulfate	K_2SO_4	Sigma-Aldrich	≥ 99.99	7778-80-5

*Purity was determined based on trace metals analysis as given by the supplier.

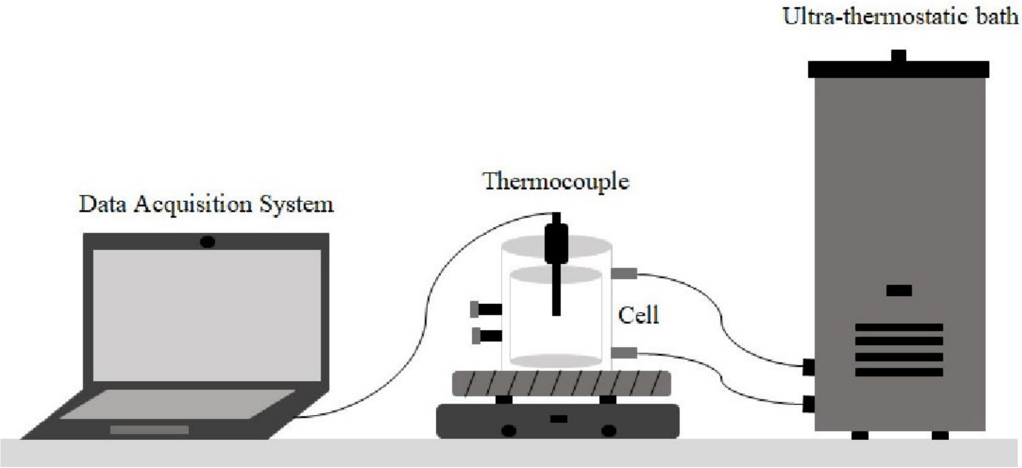

Figure 1: Apparatus used to determine the solubility of different salts in water. Adapted from Martins et al. (2021).

The saturated solution prepared with 50 mL of deionized water was filled into the glass cell and magnetic stirrer to ensure homogeneity. The temperature was measured using a data acquisition system connected to a thermocouple. After isothermal condition attainment, the solute was inserted through the lateral entrance of the glass cell in small quantities until the formation of a precipitate, ensuring the saturation of the solution. Next, the saline solution was stirred for 50 h and then allowed to settle for 24 h to ensure solution saturation (Bensouissi; Roge; Mathlouthi, 2010). The experiment was carried out at atmospheric pressure.

The solubility was gravimetrically determined after soluble solids quantification on an analytical balance accurate to 0.01 g (AUX220, Shimadzu, Japan). Three aliquots of approximately 10 mL of the supernatant solution were removed from the cell top with the help of a syringe to avoid carrying the precipitate. Then, the samples were placed on glass plates and dried in a vacuum oven (model TE-395, Tecnal, Brazil) at 353.15 K until constant mass.

Mathematical Modeling

Empirical mathematical models were adjusted to the observed solubility data as a function of temperature ranging from 275.15 to 363.15 K, aiming at predicting solubility over this temperature range. The models used were polynomial (first- to fifth-degree) Equation 1 and exponential Equation 2 similar to the one used by Martins et al. (2021). The sample standard deviation of the experimental data was calculated Equation 3. OriginPro 8.0 software (OriginLab Corporation, Northampton, MA, USA) was applied to solve the nonlinear mathematical regressions.

$$S = A + BT + CT^2 + DT^3 + ET^4 + FT^5 \tag{1}$$

$$S = \gamma_1 + \gamma_2 \exp\left(\gamma_a T\right) \tag{2}$$

$$dp = \sqrt{\frac{\sum\left(S_i - \overline{S}\right)^2}{n-1}} \tag{3}$$

In Equation 1, 2 and 3, S is the solubility [g of salt·(100 g of solution)$^{-1}$], β_1, β_2, β_3, β_4, β_5, β_6, γ_1, γ_2, and γ_3 are model parameters, T is the temperature (K), *dp* is sample standard deviation, S is solubility, $\overline{S}$ is average solubility and n is number of samples.

The evaluation criteria to determine the best fitted model were the adjusted coefficient of determination (R_{adj}^2) and the mean relative error (MRE) Equation 4.

$$MRE(\%) = \left(\frac{100}{n}\right)\sum_{i=1}^{n} \frac{\left|Y_i - Y_i^*\right|}{Y_i^*} \tag{4}$$

In Equation 4, Y_i and are the predicted and observed values, respectively, and n is the number of experiments.

Statistical Analysis

Solubility results are presented as the mean values ± standard deviation of three replicates. Data were analyzed statistically using analysis of variance (ANOVA), and mean values were compared by Tukey's test ($p < 0.05$).

RESULTS AND DISCUSSION

Solubility data

The solubilities of saturated solutions of LiBr, LiCl, LiI, $MgCl_2$, NaI, K_2CO_3, $Mg(NO_3)_2$, NaBr, KI, NaCl, $(NH_4)_2SO_4$, KCl, KNO_3, and K_2SO_4 as a function of temperature are presented in Table 2. The solubility results ranged from 7.39 to 80.41 [g of salt·(100 g of solution)$^{-1}$] and are also expressed in two other units, molarity [(mol of salt·(mol of solution)$^{-1}$] and molality [mol of salt·(kg of water)$^{-1}$] (Tables S1 to S11 - supplementary material).

Among the 14 salts studied, six presented higher solubility in water: lithium iodide (LiI), sodium iodide (NaI), lithium bromide (LiBr), magnesium nitrate ($Mg(NO_3)_2$), potassium iodide (KI), and potassium nitrate (KNO_3). Three of them exhibited lower water solubilities, potassium sulfate (K_2SO_4), sodium chloride (NaCl), and calcium chloride (KCl). Potassium sulfate (K_2SO_4) revealed the lowest ($p<0.05$) water solubility when compared to other saline solutions. Sodium iodide (NaI) had the highest water solubility in the range from 275.15 to 343.15 K, and lithium iodide (LiI) from 353.15 to 363.15 K, according to the statistical analysis ($p<0.05$).

Literature reports mostly address salt solubilities in aqueous and alcoholic media (Pinho; Macedo, 1996; Wagner et al., 1998) under salt restriction (Farelo; Brachel and Offermann 1993; Pinho; Macedo, 2005) and often refer to the salts NaCl, NaBr, and KCl. The observed solubility data differ from those found by Pinho and Macedo (2005) by a maximum of 5.0% for the salts NaBr, NaCl and KCl. However, comparison among solubility results should be done with caution due to the low similarity between temperature and solvent conditions used in the tests.

Intermolecular interactions between water molecules affect salt solubility. If ion-dipole interactions between the water molecules and the salt ions are, on average, stronger than electrostatic attraction between the salt ions, salt dissociation occurs (Bensouissi; Roge; Mathlouthi, 2010). On the other hand, solubilization considerably increases the total configurational entropy in the system. It is related to the number of alternatives that the available energy can be distributed among the particles contained in a given system. When the total configurational entropy is high, it tends to increase the solubility of the salt in water (Fisicaro et al., 2008; Graeser et al., 2010).

In addition, solubility can be explained by the Law of Matching Water Affinities theory, which is associated with Hofmeister's effects. Figure 2 shows the classification of the Hofmeister series ions as kosmotropic or chaotropic following the hydration degree.

Table 2: Saturation condition (S) of saline solutions at different temperatures (T) (mean ± standard deviation).[a]

	g of salt . (100 g of solution)$^{-1}$													
T(K)	LiBr	LiCl	LiI	$MgCl_2$	NaI	K_2CO_3	$Mg(NO_3)_2$	NaBr	KI	NaCl	$(NH_4)_2SO_4$	KCL	KNO_3	K_2SO_4
275.15	58.173±0.188^{hB}	39.704±0.134^{kG}	58.663±0.026^{kB}	33.601±0.067^{iH}	61.322±0.162^{iA}	51.496±0.351^{gD}	38.573±1.671^{hG}	44.965±0.128^{iE}	56,676±0.153^{kC}	26.527±0.057^{dI}	41.244±0.140^{eF}	22.148±0.535^{hJ}	12.841±0.202^{jK}	7.385±0.178^{jL}
278.15	58.973±0.185^{gB}	40.525±0.112^{jG}	58.991±0.028^{jB}	34.097±0.052^{hI}	61.250±0.073^{iA}	50.642±0.261^{fgD}	38.868±1.557^{hH}	45.319±0.016^{hE}	57,035±0.074^{jC}	26.369±0.080^{cdJ}	42.202±0.162^{eF}	22.733±0.550^{hK}	14.560±0.256^{jL}	7.776±0.188^{ijM}
283.15	60.651±0.136^{fAB}	43.090±0.145^{iF}	59.554±0.042^{iB}	34.484±0.173^{hI}	61.317±0.118^{iA}	51.833±0.908^{fgD}	39.692±0.452^{hH}	46.578±0.138^{gE}	57,796±0.106^{iC}	26.098±0.567^{cdJ}	41.435±0.112^{eG}	23.246±0.577^{hK}	17.390±0.413^{iL}	8.424±0.209^{iM}
293.15	62.668±0.114^{eA}	44.844±0.113^{hF}	60.971±0.021^{hB}	35.206±0.074^{gI}	62.927±0.106^{hA}	52.364±0.380^{efgD}	40.956±0.038^{ghH}	48.252±0.064^{fE}	59,291±0.056^{hC}	26.432±0.058^{cdJ}	42.823±0.535^{deG}	25.401±0.458^{gK}	24.115±0.293^{hL}	9.968±0.180^{hM}
303.15	65.952±0.061^{dA}	45.445±0.111^{gF}	62.995±0.041^{gB}	35.856±0.086^{fH}	65.604±0.062^{gA}	53.245±0.410^{defD}	42.606±1.301^{fgG}	49.896±0.115^{eE}	60,541±0.597^{gC}	26.789±0.540^{cdJ}	43.140±1.245^{deG}	27.361±0.024^{fJ}	30.425±0.666^{gI}	11.456±0.010^{gK}
313.15	67.682±0.100^{cA}	47.518±0.067^{fF}	64.965±0.035^{fB}	36.509±0.050^{eH}	67.966±0.334^{fA}	53.320±0.219^{defD}	44.979±0.434^{efG}	51.381±0.019^{dE}	61,793±0.052^{fC}	26.383±0.470^{bcdJ}	44.731±1.344^{cdG}	28.905±0.446^{efI}	37.599±0.727^{fH}	12.794±0.198^{fK}
323.15	67.697±0.041^{cB}	48.749±0.074^{eG}	65.946±0.019^{eC}	37.176±0.255^{dI}	70.545±0.242^{eA}	54.269±1.230^{cdeE}	45.995±0.441^{deH}	52.303±0.258^{cF}	62,956±0.264^{eD}	26.414±0.207^{bcdK}	45.622±0.758^{bcH}	30.223±0.122^{deJ}	45.971±0.415^{eH}	14.145±0.057^{eL}
333.15	67.846±0.175^{cB}	49.698±0.136^{dG}	66.097±0.008^{dC}	37.577±0.093^{dJ}	72.696±0.103^{dA}	55.108±0.408^{cdE}	48.055±0.171^{cdH}	52.843±0.170^{cF}	63,945±0.254^{dD}	26.516±0.081^{abcdL}	46.209±0.662^{bcI}	31.463±0.818^{cdK}	52.159±0.200^{dF}	15.676±0.408^{dM}
343.15	69.813±0.018^{bB}	51.255±0.114^{cF}	68.936±0.006^{cB}	38.532±0.184^{cH}	74.150±0.012^{cA}	56.260±0.924^{bcD}	50.058±0.132^{bcF}	53.345±0.076 ^{bE}	64,781±0.067^{cC}	27.558±0.129^{abcJ}	47.711±1.219^{abG}	32.739±0.087^{bcI}	56.791±0.263^{cD}	16.569±0.044^{cK}
353.15	69.647±0.165^{bC}	53.098±0.147^{bG}	80.020±0.029^{bA}	39.558±0.190^{bJ}	75.149±0.103^{bD}	57.471±0.953^{abF}	51.705±0.237^{bH}	53.382±0.124^{bG}	65,651±0.140^{bD}	27.776±0.145^{abL}	48.707±0.153^{aI}	33.880±0.875^{abK}	62.991±0.718^{bE}	17.739±0.458^{bM}
363.15	70.59±0.198^{aC}	54.046±0.087^{aF}	80.414±0.069^{aA}	40.548±0.263^{aH}	75.542±0.055^{aB}	59.039±1.263^{aE}	70.178±1.783^{aC}	53.854±0.113^{aF}	66,524±0.103^{aD}	27.345±0.732^{aJ}	49.640±0.602^{aG}	34.412±0.806^{aI}	66.411±1.978^{aD}	18.583±0.435^{aK}

Lithium bromide (LiBr), Lithium chloride (LiCl), Lithium iodide (LiI), Magnesium chloride ($MgCl_2$), Sodium iodide (NaI), Potassium carbonate (K_2CO_3), Magnesium nitrate ($Mg(NO_3)_2$), Sodium bromide (NaBr), Potassium iodide (KI), Sodium chloride (NaCl), Ammonium sulfate ($(NH_4)_2SO_4$), Potassium chloride (KCl), Potassium nitrate (KNO_3), Potassium sulfate (K_2SO_4).

Means and standard deviations followed by different uppercase letters in the same row and different lowercase letters in the same column indicate significant differences according to Analysis of Variance and post-hoc Tukey's test ($\alpha = 0.05$). [a]Standard uncertainties are u(T)=0.20K, u(P)=0.10kPa, electrical conductivity u(σ)=0.004 μS.cm^{-1}, thermal conductivity u(λ)= 0.002 W.m^{-1}.K^{-1} and mass of solute u(m)=0.01g.

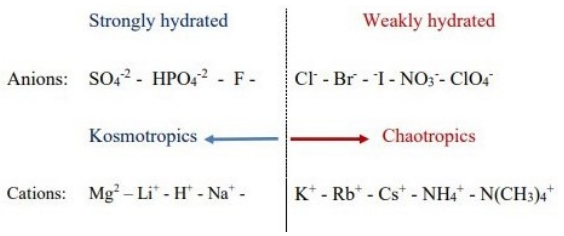

Figure 2: Kosmotropic and chaotropic ions according to the Hofmeister series. Adapted from Yang (2009).

Kosmotropic ions exhibited a strong bond with water and a high degree of hydration (Yang, 2009); chaotropic ions presented weakly bound with water and a low degree of hydration. The ion size also influences their interaction with water molecules. Larger ions have loosely bound water molecules around them, and the smaller ions have an inverse behavior (Kunz; Neueder, 2009).

Temperature changes affected solubility, as observed in Table 2. Solubility increased ($p<0.05$) with increasing temperature for all saturated saline solutions, corroborating the behavior reported by Pinho and Macedo (2005). High temperatures are a consequence of the higher kinetic energy of the molecules and ions. We also verified that the temperature increase promoted great stability in solubility for salts, with low solubilities, and large modifications in solubility for salts with higher solubilities. The amount of solute can also influence the solubility; the larger the amount of solute is, the greater the changes in hydrogen interactions of water molecules. The literature pointed out that some solute characteristics could explain the high solute solubility in water, such as low molecular mass, less complex chemical structures, and resistance to chemical reactions. Thus, solvent-mixed solutions are used to enhance solute solubility (Demirbas, 2004; Martínez; Peña; Bustamante, 2011).

The salt amounts to prepare 100 g of the saturated aqueous solution of the 14 studied types of salts are presented in Table 2. Greenspan (1977) presents data on equilibrium relative humidity for several saturated saline solutions. The division of these values by 100 results in the water activity data. Consequently, environments for isothermal experiments can be formed with safety from the solubility (Table 2) and water activity (Table 3) data. Thus, we present a list of salts used to determine moisture sorption isotherms of foods over a wide temperature range (275.15 to 363.15 K), including 11 temperature values.

Table 3: Water activity (a_w) of different saturated saline solutions at different temperatures (T).[a]

T(K)	LiBr	LiCl	LiI	$MgCl_2$	NaI	K_2CO_3	$Mg(NO_3)_2$	NaBr	KI	NaCl	$(NH_4)_2SO_4$	KCl	KNO_3	K_2SO_4
275.15	0.0762	0.1124	---	0.3363	---	0.4313	0.5975	---	---	0.7556	0.8233	0.8823	0.9764	0.9865
278.15	0.0743	0.1126	0.2168	0.3360	0.4242	0.4313	0.5886	0.6351	0.7330	0.7565	0.8242	0.8767	0.99627	0.9848
283.15	0.0714	0.1129	0.2061	0.3347	0.4183	0.4314	0.5736	0.6215	0.7211	0.7567	0.8206	0.8677	0.9596	0.9818
293.15	0.0661	0.1131	0.1856	0.3307	0.3965	0.4316	0.5438	0.5914	0.6990	0.7547	0.8134	0.8511	0.9462	0.9759
303.15	0.0616	0.1128	0.1657	0.3244	0.3615	0.4317	0.5140	0.5603	0.6789	0.7509	0.8063	0.8362	0.9231	0.9700
313.15	0.0580	0.1121	0.1455	0.3160	0.3288	---	0.4842	0.5317	0.6609	0.7468	0.7991	0.8232	0.8903	0.9641
323.15	0.0553	0.1110	0.1238	0.3054	0.2921	---	0.4544	0.5093	0.6449	0.7443	0.7920	0.8120	0.8478	0.9582
333.15	0.0533	0.1095	0.0998	0.2926	0.2595	---	---	0.4966	0.6311	0.7450	---	0.8025	---	---
343.15	0.0523	0.1075	0.0723	0.2777	0.2357	---	---	0.4970	0.6193	0.7506	---	0.7949	---	---
353.15	0.0520	0.1051	---	0.2605	0.2252	---	---	0.5143	0.6097	0.7629	---	0.7890	---	---
363.15	0.0526	0.1023	---	0.2412	0.2325	---	---	---	0.6021	---	---	0.7850	---	---

Adapted from Greenspan (1977). Lithium bromide (LiBr), Lithium chloride (LiCl), Lithium iodide (LiI), Magnesium chloride ($MgCl_2$), Sodium iodide (NaI), Potassium carbonate (K_2CO_3), Magnesium nitrate ($Mg(NO_3)_2$), Sodium bromide (NaBr), Potassium iodide (KI), Sodium chloride (NaCl), Ammonium sulfate ($(NH_4)_2SO_4$), Potassium chloride (KCl), Potassium nitrate (KNO_3), Potassium sulfate (K_2SO_4). [a]Greenspan (1977) did not show the standard uncertainties.

The temperature range studied includes the industrial conditions used for drying and storing most food systems, enabling obtaining food sorption isotherms. These isotherms, in turn, are used to solve problems in food engineering and food science, such as in the storage of industrial waste, such as papaya seed (Rosa et al., 2021), melon seed (Mallek-Ayadi; Bahloul; Kechaou, 2020), cassava bagasse (Polachini et al., 2016), and products such as cooked ham (Barretto et al., 2018), chia seed (Arslan-Tontul, 2020), pork liver (Sánchez-Torres et al., 2021), wheat malt (Silva et al., 2021) and dry-cured ham (Leonardo Betiol et al., 2020).

Mathematical modeling

Linear, second-order to fifth-order polynomial, and exponential mathematical models were fitted with experimental data. These types of models are considered simple and easy to apply in calculations involving unit operations. Thus, they are frequently applied in thermophysical property studies of food systems, such as concentrated grape juice (Evangelista et al., 2020), Malay rose apple pulp (Fontan, 2018), and aqueous solutions of sodium chloride (Carvalho et al., 2015), sucrose-maltitol (Martins et al., 2021), and isomaltulose (Do Carmo et al., 2022).

A general mathematical model to predict the solubility of all saline solutions was not obtained due to the different salt behavior and performance on the temperature increase; thus, five mathematical models are proposed to represent the solubility behavior of the tested salts.

The parameters and the adjustments of the best polynomial model for each salt ($R_{adj}^2 \geq 0.9094$ and RMSE ≤ 2.8770) are shown in Table 4. The fit of the other models to the experimental data is available in the supplementary material (Table S15). The graphical representation of the data with the best-fitted model is presented in Figure 3.

For LiI and NaCl solutions, the mathematical models exhibited poor representation of the experimental data; therefore, the solubility values for both types of salts can be determined using the observed values in Table 2. Linear interpolation can be applied if necessary.

Solubility data for saturated saline solutions are not easily found in the literature and are helpful in isotherm studies, analysis of evaporation mechanisms (Kuznetsov et al., 2018), preparation of activated charcoal (Yuliusman et al., 2020), meat salting processes (Cárcel et al., 2007), and in the project and design of equipment such as a water absorption machine of single-stage lithium bromide (LiBr) (Florides et al., 2003).

Table 4: Fitting parameters of the fifth-degree polynomial model to describe the solubility (*S*) of saturated salt solutions.

Parameters	LiBr	LiCl	LiI	$MgCl_2$	NaI	K_2CO_3	$Mg(NO_3)_2$	NaBr	KI	NaCl	$(NH4)_2SO_4$	KCl	KNO3	K_2SO_4
A	-7148.21714	-6941.75942	372632.36617	-342.63757	1162.73816	66.95652	-12.24708	-135.55158	-22.46057	79143.0481	85.65506	-220.90708	1524.59032	-14.49529
B	87.32071	85.36493	-5833.17375	3.51641	-10.92939	-0.1668	0.1815	1.07486	0.42096	-1272.0714	-0.35914	1.86361	-16.00393	-0.1067
C	-0.39731	-0.39129	36.40708	-0.01104	0.03554	$3.95071 \cdot 10^{-4}$	-	-0.00153	$-4.85213 \cdot 10^{-4}$	8.1631	$7.20504 \cdot 10^{-4}$	-0.00473	0.05445	0.00109
D	$8.0481 \cdot 10^{-4}$	$7.96698 \cdot 10^{-4}$	-0.11323	$1.17331 \cdot 10^{-5}$	$-3.7685 \cdot 10^{-5}$	-	-	-	-	-0.0261	-	$4.2254 \cdot 10^{-6}$	$-5.90784 \cdot 10^{-5}$	$-1.489 \cdot 10^{-6}$
E	$-6.11704 \cdot 10^{-7}$	$-6.07027 \cdot 10^{-7}$	$1.7546 \cdot 10^{-4}$	-	-	-	-	-	-	$4.1732 \cdot 10^{-5}$	-	-	-	-
F	-	-	$-1.08375 \cdot 10^{-7}$	-	-	-	-	-	-	$-2.6594 \cdot 10^{-8}$	-	-	-	-
R^2	0.9734	0.9915	0.9094	0.9966	0.9990	0.9378	0.9871	0.9993	0.9996	0.9127	0.9804	0.9995	0.9994	0.99991
MRE	0.7508	0.5646	1.9283	0.2258	0.3341	0.5744	2.8770	0.3044	0.0730	0.6130	0.9755	0.0589	1.2492	0.5169

Lithium bromide (LiBr), Lithium chloride (LiCl), Lithium iodide (LiI), Magnesium chloride ($MgCl_2$), Sodium iodide (NaI), Potassium carbonate (K_2CO_3), Magnesium nitrate ($Mg(NO_3)_2$), Sodium bromide (NaBr), Potassium iodide (KI), Sodium chloride (NaCl), Ammonium sulfate ($(NH_4)_2SO_4$), Potassium chloride (KCl), Potassium nitrate (KNO_3), Potassium sulfate (K_2SO_4).

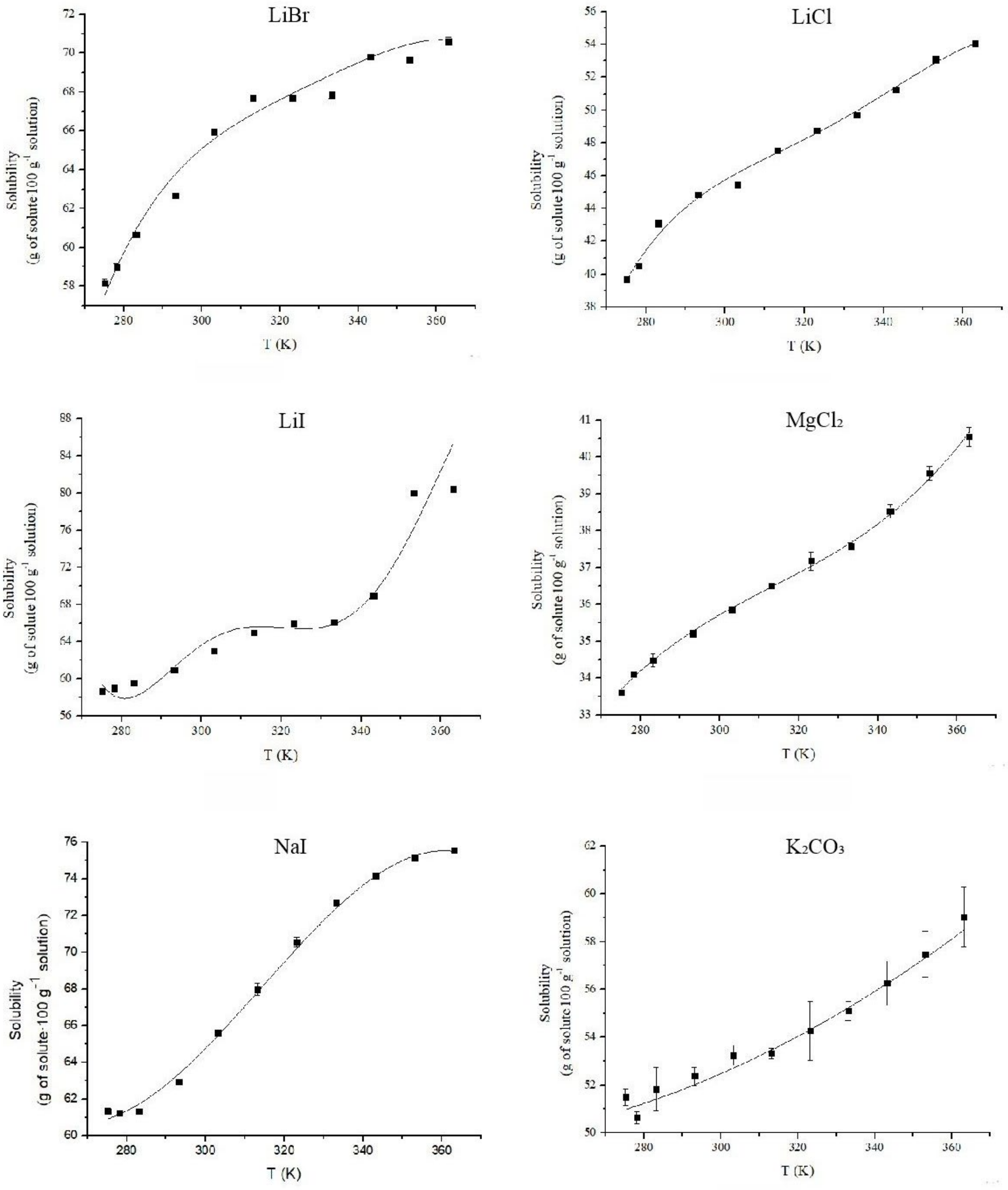

Continue...

Figure 3: Salt solubility (S) at different temperatures (T). Points: solubility mean values. Vertical bars: standard deviations. Lines: best-fitted model. Saturated aqueous solutions of LiBr, LiCl, LiI, $MgCl_2$, NaI, K_2CO_3, $Mg(NO_3)_2$, NaB, KI, NaCl, $(NH_4)_2SO_4$, KCl, KNO_3, and K_2SO_4.

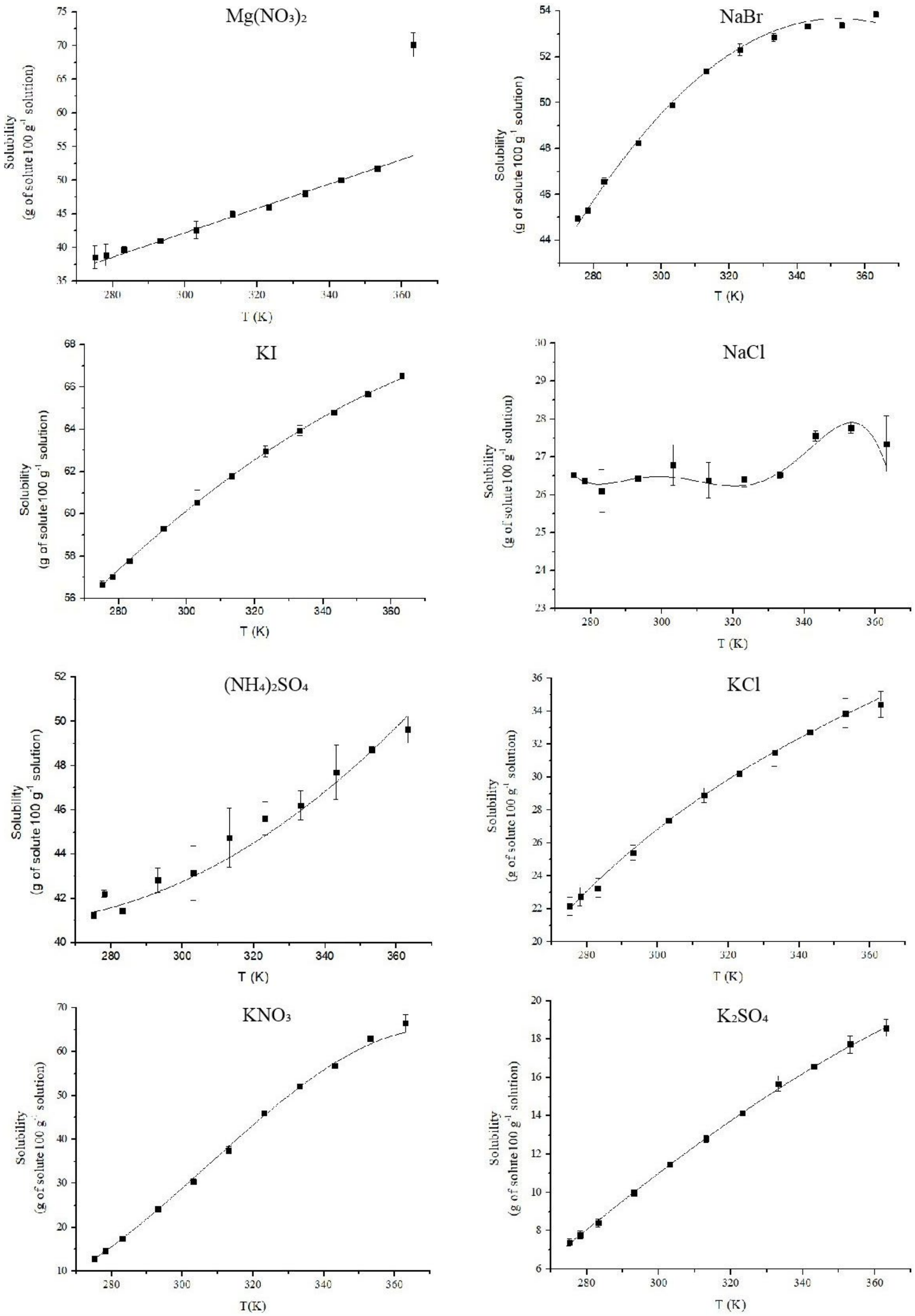

Figure 3: Continuation.

CONCLUSIONS

Solubility and water activity data of saline solutions are useful for determining food sorption isotherms. The LiI revealed the highest solubility in aqueous solutions, and K_2SO_4 had the lowest solubility. The salts showed dependence and differentiated behavior in the temperature range studied. Furthermore, the water activity of saline solutions decreases with increasing temperature. A general mathematical model was not proposed to predict solubility data, as each salt had specific characteristics, making the solubility database essential.

AUTHOR CONTRIBUTION

Conceptual idea: Martins, M.J.N.; Sanches, M.A.R.; Polachini, T.C.; Oliveira, E.B.; Reis Coimbra, J.S.; Telis-Romero, J., Methodology design: Martins, M.J.N.; Sanches, M.A.R.; Polachini, T.C.; Oliveira, E.B.; Reis Coimbra, J.S.; Telis-Romero, J., Data collection: Polachini, T.C.; Martins, M.J.N.; Sanches, M.A.R., Data analysis and interpretation: Martins, M.J.N.; Sanches, M.A.R.; Polachini, T.C.; Oliveira, E.B.; Reis Coimbra, J.S.; Telis-Romero, J., Writing and editing: Martins, M.J.N.; Sanches, M.A.R.; Polachini, T.C.; Oliveira, E.B.; Reis Coimbra, J.S.; Telis-Romero, J.

ACKNOWLEDGMENTS

This study was financed in part by the Coordenação de Aperfeiçoamento de Pessoal de Nível Superior - Brasil (CAPES) - Finance Code 001. The authors are also grateful to the Conselho Nacional de Desenvolvimento Científico e Tecnológico (CNPq, Brazil) for funding the productivity grants of J. Telis-Romero (308567/2017-0).

REFERENCES

ALBERTO ALVES-JUNIOR, C. et al. Solubilidade de cloreto de sódio e seus sais substitutos para utilização na indústria de alimentos. Ciência e Tecnologia de Alimentos: Pesquisa e Práticas Contemporâneas, 1(1):551-557, 2021.

ARSLAN-TONTUL, S. Moisture sorption isotherm, isosteric heat and adsorption surface area of whole chia seeds. LWT, 119:108859, 2020.

BAMPI, M. et al. Influence of vacuum application, acid addition and partial replacement of NaCl by KCl on the mass transfer during salting of beef cuts. LWT: Food Science and Technology, 74:26-33, 2016.

BARRETTO, T. L. et al. Water sorption isotherms of cooked hams as affected by temperature and chemical composition. Food Science and Technology, 39(3):677-683, 2018.

BENSOUISSI, A.; ROGE, B.; MATHLOUTHI, M. Effect of conformation and water interactions of sucrose, maltitol, mannitol and xylitol on their metastable zone width and ease of nucleation. Food Chemistry, 122(2):443-446, 2010.

BHATTACHAR, S. N.; DESCHENES, L. A.; WESLEY, J. A solubility: It's not just for physical chemists. Drug Discovery Today, 11(21-22):1012-1018, 2006.

CÁRCEL, J. A. et al. High intensity ultrasound effects on meat brining. Meat Science, 76(4):611-619, 2007.

CARVALHO, R. et al. Physicothermal properties of aqueous sodium chloride solutions. Journal of Food Process Engineering, 38(3):234-242, 2015.

CHIRIFE, J.; RESNIK, S. L. Unsaturated solutions of sodium chloride as reference sources of water activity at various temperatures. Journal of Food Science, 49(6):1486-1488, 1984.

DEMIRBAS, A. Adsorption of lead and cadmium ions in aqueous solutions onto modified lignin from alkali glycerol delignication. Journal of Hazardous Materials, 109(1-3):221-226, 2004.

DO CARMO, J. R. et al. Properties of isomaltulose (Palatinose®): An emerging healthy carbohydrate: Effect of temperature and solute concentration. Journal of Molecular Liquids, 347:118304, 2022.

EVANGELISTA, R. R. et al. Determination of the rheological behavior and thermophysical properties of malbec grape juice concentrates (*Vitis vinifera*). Food Research International, 137:109431, 2020.

FARELO, F.; VON BRACHEL, G.; OFFERMANN, H. Solid-liquid equilibria in the ternary system NaCl-KCL-H_2O. The Canadian Journal of Chemical Engineering, 71(1):141-146, 1993.

FILIPPA, M. A.; GASULL, E. I. Experimental determination of Naproxen solubility in organic solvents and aqueous binary mixtures: Interactions and thermodynamic parameters relating to the solvation process. Journal of Molecular Liquids, 198:78-83, 2014.

FISICARO, E. et al. Entropy changes in aqueous solutions of non-polar substances and in bio-complex formation. Journal of Solution Chemistry, 37:487-501, 2008.

FLORIDES, G. A. et al. Design and construction of a LiBr: Water absorption machine. Energy Conversion and Management, 44(15):2483-2508, 2003.

FONTAN, R. C. I. et al. Composition and thermophysical properties of malay rose apple pulp. International Food Research Journal, 25(3):1067-1073, 2018.

FREITAS, M. L. F. et al. Sorption isotherms and thermodynamic properties of grated parmesan cheese. International Journal of Food Science & Technology, 51(1):250-259, 2016.

GRAESER, K. A. et al. The role of configurational entropy in amorphous systems. Pharmaceutics, 2(2):224-244, 2010.

GREENSPAN, L. Humidity fixed points of binary saturated aqueous solutions. Journal of Research of the National Bureau of Standards: Section A. Physics and Chemistry, 81(1):89-96, 1977.

INGUGLIA, E. S. et al. Salt reduction strategies in processed meat products: A review. Trends in Food Science & Technology, 59:70-78, 2017.

KUNZ, W; NEUEDER, R. An attempt of a general overview. In: KUNZ, W. Specific ion effects. World Scientific: Singapore, p.3-54, 2009.

KUZNETSOV, G. V. et al. Evaporation modes of LiBr, CaCl2, LiCl, NaCl aqueous salt solution droplets on aluminum surface. International Journal of Heat and Mass Transfer, 126:161-168, 2018.

LAROTONDA, F. D. S. et al. Hygroscopicity and water vapor permeability of kraft paper impregnated with starch acetate. Journal of Food Engineering, 71(4):394-402, 2005.

LEONARDO BETIOL, L. F. et al. Influence of temperature and chemical composition on water sorption isotherms for dry-cured ham. LWT: Food Science and Technology, 123:109112, 2020.

MALI, S. et al. Water sorption and mechanical properties of cassava starch films and their relation to plasticizing effect. Carbohydrate Polymers, 60(3):283-289, 2005.

MALLEK-AYADI, S.; BAHLOUL, N.; KECHAOU, N. Mathematical modelling of water sorption isotherms and thermodynamic properties of *Cucumis melo* L. seeds. LWT: Food Science and Technology, 131:109727, 2020.

MARTÍNEZ, F.; PEÑA, M. Á.; BUSTAMANTE, P. Thermodynamic analysis and enthalpy–entropy compensation for the solubility of indomethacin in aqueous and non-aqueous mixtures. Fluid Phase Equilibria, 308(1-2):98-106, 2011.

MARTINS, M. J. N. et al. Thermophysical properties of carbohydrate solutions: Correlation between thermal and transport properties. Journal of Food Process Engineering, 43(9):e13483, 2020.

MARTINS, M. J. N. et al. Transport properties of saturated sucrose and maltitol solutions as affected by temperature. Journal of Molecular Liquids, 336:116254, 2021.

PINHO, S. P.; MACEDO, E. A. Representation of salt solubility in mixed solvents: A comparison of thermodynamic models. Fluid Phase Equilibria, 116(1-2):209-216, 1996.

PINHO, S. P.; MACEDO, E. A. Solubility of NaCl, NaBr, and KCl in water, methanol, ethanol, and their mixed solvents. Journal of Chemical and Engineering Data, 50(1):29-32, 2005.

POLACHINI, T. C. et al. Water adsorption isotherms and thermodynamic properties of cassava bagasse. Thermochimica Acta, 632:79-85, 2016.

RAMYA, V.; JAIN, N. K. A Review on osmotic dehydration of fruits and vegetables: An integrated approach. Journal of Food Process Engineering, 40(3):e12440, 2017.

RIBEIRO SANCHES, M. A. et al. Development, characterization and optimization of biopolymers films based on starch and flour from jabuticaba (*Myrciaria cauliflora*) peel. Food Chemistry, 343:128430, 2021.

ROSA, D. P. et al. Water sorption properties of papaya seeds (*Carica papaya* L.) formosa variety: An assessment under storage and drying conditions. LWT, 138:110458, 2021.

SANCHES, M. A. R. et al. Technological and diffusion properties in the wet salting of beef assisted by ultrasound. LWT, 149:112036, 2021.

SÁNCHEZ-TORRES, E. A. et al. Water desorption isotherms of pork liver and thermodynamic properties. LWT, 149:111857, 2021.

SILVA, K. S. et al. Sorption isotherms and thermodynamic properties of wheat malt under storage conditions. Journal of Food Process Engineering, 44(9):e13784, 2021.

WAGNER, K. et al. Solubilities of sodium chloride in organic and aqueous-organic solvent mixtures. Journal of Chemical & Engineering Data, 43(5):871-875, 1998.

YANG, Z. Hofmeister effects: An explanation for the impact of ionic liquids on biocatalysis. Journal of Biotechnology, 144(1):12-22, 2009.

YULIUSMAN, Y. et al. Utilization of durian shell waste in the preparation of activated carbon by using K2CO3 as chemical activator. AIP Conference Proceedings, 2255(1):060027, 2020.

ZHANG, D. et al. Study on the mechanism of KCl replacement of NaCl on the water retention of salted pork. Food Chemistry, 332:127414, 2020.